



## ■ SPINE

# Extracellular vesicles derived from mesenchymal stem cells containing microRNA-381 protect against spinal cord injury in a rat model via the BRD4/WNT5A axis

**X. Jia,  
G. Huang,  
S. Wang,  
M. Long,  
X. Tang,  
D. Feng,  
Q. Zhou**

From The People's Hospital of Jiayang City, Jiayang, China

**Aims**

Non-coding microRNA (miRNA) in extracellular vesicles (EVs) derived from mesenchymal stem cells (MSCs) may promote neuronal repair after spinal cord injury (SCI). In this paper we report on the effects of MSC-EV-microRNA-381 (miR-381) in a rodent model of SCI.

**Methods**

In the current study, the luciferase assay confirmed a binding site of bromodomain-containing protein 4 (BRD4) and Wnt family member 5A (WNT5A). Then we detected expression of miR-381, BRD4, and WNT5A in dorsal root ganglia (DRG) cells treated with MSC-isolated EVs and measured neuron apoptosis in culture by terminal deoxynucleotidyl transferase dUTP nick end labeling (TUNEL) staining. A rat model of SCI was established to detect the in vivo effect of miR-381 and MSC-EVs on SCI.

**Results**

We confirmed an interaction between miR-381 and BRD4, and showed that miR-381 overexpression inhibited the expression of BRD4 in DRG cells as well as the apoptosis of DRG cells through WNT5A via activation of Ras homologous A (RhoA)/Rho-kinase activity. Moreover, treatment of MSC-EVs rescued neuron apoptosis and promoted the recovery of SCI through inhibition of the BRD4/WNT5A axis.

**Conclusion**

Taken altogether, miR-381 derived from MSC-EVs can promote the recovery of SCI through BRD4/WNT5A axis, providing a new perspective on SCI treatment.

**Cite this article:** *Bone Joint Res* 2021;10(5):328–339.

**Keywords:** Mesenchymal stem cell, Extracellular vesicle, miR-381, Dorsal root ganglia, Spinal cord injury

**Article focus**

- We aimed to identify the specific role of microRNA-381 (miR-381) from mesenchymal stem cell-derived extracellular vesicles (MSC-EVs) in spinal cord injury (SCI) recovery and its functioning mechanism.
- The findings of miR-381 from MSC-EVs were verified in dorsal root ganglia (DRG) cells and rat model of SCI.
- miR-381 derived from MSC-EVs can promote the recovery of SCI through bromodomain-containing protein 4

(BRD4)/Wnt family member 5A (WNT5A) axis.

**Key messages**

- BRD4 promoted the expression of WNT5A via binding to the promoter of WNT5A.
- Extracellular vesicles (EVs) derived from MSCs promoted the recovery of SCI.
- EV-derived miR-381 promoted the recovery of SCI by inhibiting WNT5A.

Correspondence should be sent to Qingzhong Zhou; email: spinalzhou@163.com

doi: 10.1302/2046-3758.105.BJR-2020-0020.R1

*Bone Joint Res* 2021;10(5):328–339.

## Strengths and limitations

- The underlying mechanism of miR-382 from MSC-EVs could provide a novel insight into treatment for and recovery from SCI.
- The current technique limits the efficiency of EV isolation in the present study.

## Introduction

Spinal cord injury (SCI) is a frequent occurrence in modern society, due to adverse events such as vehicular crashes, falls, violence, sports, and medical/surgical accidents.<sup>1</sup> Generally, SCI proceeds from an initial mechanical injury to secondary damage from inflammation and apoptosis.<sup>2,3</sup> Early treatment can exert a positive effect on neurological recovery, but the recovery rate is still lower than would be desired, thus bringing a considerable burden of disability.<sup>4</sup> Furthermore, treatment complications can include sepsis and multiorgan failure, resulting in long-standing hospitalization or morbidity.<sup>5</sup> Emerging evidence indicates that bone marrow-carried mesenchymal stem cells (MSCs) hold considerable promise for SCI treatment.<sup>6</sup>

Extracellular vesicles (EVs) serve as vehicles for the delivery to target cells of cargos consisting of messenger RNA (mRNA), microRNA (miRNA), and long non-coding RNA, as well as diverse lipids.<sup>7</sup> Among many beneficial processes, EVs can improve the repair of bone injury through an endochondral pathway by delivery of pro-regenerative paracrine signalling factors to the site of damage.<sup>8</sup> MicroRNAs are a group of small non-coding RNAs, which are emerging as valuable biomarkers for many diseases, as well as presenting new therapeutic targets.<sup>9</sup> A recent study verified that miRNA-381 is essential for the proliferation of nerve cells during SCI by inhibiting the expression of HES1 gene, thus presenting a new potential therapeutic direction for treating SCI.<sup>10</sup> Treatment with MSC-derived exosomes modified to deliver miR-126 could reduce the injury degree, stimulate axon regeneration, and improve recovery of limb motor function following SCI in a rodent model.<sup>11</sup> Moreover, the miRNA.org database has predicted an association between bromodomain-containing protein 4 (BRD4) and miR-381. A previous study showed that BRD4 was related to the pathophysiology of neuropathic pain and HIV-related pain.<sup>12</sup> BRD4 can bind to the promoter region of Wnt family member 5A (WNT5A) in breast cancer,<sup>13</sup> which is also known to be upregulated after SCI.<sup>14</sup> Hence, we proposed to test a hypothesis that EV-encapsulated miR-381 from MSCs can promote the recovery of SCI through the inhibition of the BRD4/WNT5A axis. We tested this novel therapeutic channel using cell cultures and in SCI-model rats.

## Methods

**Ethical statement.** The animal experiments in this study were conducted under the approval of the Animal Ethics Committee in our hospital, in strict consideration of the need to minimize discomfort and animal numbers.

**Table 1.** Mesenchymal stem cell-derived extracellular vesicle treatments.

Group	Treatment
MSC-EVs-NC mimic+oe-NC	MSCs were transfected with NC mimic for six hours and then the MSCs were cultured in DMEM medium for 24 hours. With supernatant collected, EVs of MSCs were isolated. Then the MSC-EVs and lentivirus expressing oe-NC were intravenously injected into rats (n = 8).
MSC-EVs-miR-381 mimic+oe NC	MSCs were transfected with miR-381 mimic for six hours and then the MSCs were cultured in DMEM medium for 24 hours. With supernatant collected, EVs of MSCs were isolated. Then the MSC-EVs and lentivirus expressing oe-NC were intravenously injected into rats (n = 8).
MSC-EVs-miR-381 mimic+oe-BRD4	MSCs were transfected with miR-381 mimic for six hours and then the MSCs were cultured in DMEM medium for 24 hours. With supernatant collected, EVs of MSCs were isolated. Then the MSC-EVs and lentivirus expressing oe-BRD4 were intravenously injected into rats (n = 8).
MSC-EVs-miR-381 mimic+oe-WNT5A	MSCs were transfected with miR-381 mimic for six hours and then the MSCs were cultured in DMEM medium for 24 hours. With supernatant collected, EVs of MSCs were isolated. Then the MSC-EVs and lentivirus expressing oe-WNT5A were intravenously injected into rats (n = 8).

BRD4, bromodomain-containing protein 4; DMEM, Dulbecco's modified Eagle's medium; EV, extracellular vesicle; miRNA-381, microRNA-381; MSC, mesenchymal stem cell; oe-NC, overexpression negative control; WNT5A, Wnt family member 5A.

**Spinal cord injury model in rats.** A total of 56 Sprague-Dawley (SD) rats (male, 6 to 8 weeks, 180 g to 205 g) were raised in separate cages, with ad libitum access to food and water. The rats were anaesthetized with 1% (w/v) pentobarbital sodium (40 mg/kg) and operated to produce the SCI. Under surgical anaesthesia, we exposed the T9 lamina of each rat and excised its surrounding skin and muscle to expose the vertebral plate and spinous process. These T9 structures were removed by placing a mosquito clamp to expose the spinal cord, which was held in place for one minute to establish a moderately severe crush injury model. In the control group, the T9 lamina of the rats was excised without compression injury.

**Animal treatment.** With eight normal rats taken as normal controls, the remaining rats (n = 48) were subjected to different treatments for SCI. Three days before spinal cord percussion, the 48 treatment rats were intravenously injected with miR-381 agomir, EVs from MSCs transfected with negative control mimic (MSC-EV-NC mimic) or miR-381 mimic (MSC-EV-miR-381 mimic), lentivirus expressing overexpression of BRD4 (oe-BRD4), oe-WNT5A, or empty vectors (n = 8 per treatment group; Table 1).

During the establishment of the SCI model, we applied the Basso, Beattie and Bresnahan locomotor rating scale (BBB scale)<sup>15</sup> to evaluate the neural function of the injured spinal cord, and ultimately harvested the injured spinal cord tissue, whereupon we counted the number of neurones after Nissl staining. Haematoxylin-eosin staining (HE staining) was used to investigate the

**Table II.** Primer sequences.

Target	Sequence
BRD4	F: 5'-GGACGAGGGAGGAAAGAAACA-3' R: 5'-AGGAAAGGGGTGAGTTGTGG-3'
WNT5A	F: 5'-ACCACATGCAGTACATCGGAG-3' R: 5'-ACCACATGCAGTACATCGGAG-3'
miR-381	F: 5'-CGTGAATGATAGTGAGGAAC-3' R: 5'-GTGAACGATTGCCACACACA-3'
U6	F: 5'-GCTTCGGCAGCACATATACTAAAAT-3' R: 5'-CGCTTCAGAAATTCGCTGTCCAT-3'
GAPDH	F: 5'-TGGCCTTCCGTGTTCTCTAC-3' R: 5'-GAGTGTGCTGTTGAAGTC-3'

BRD4, bromodomain-containing protein 4; F, forward; GAPDH, glyceraldehyde 3-phosphate dehydrogenase; miR-381, microRNA-381; R, reverse; WNT5A, Wnt family member 5A.

histopathological differences between treatment groups. The expression of miR-381, BRD4, and WNT5A was detected in tissue samples by reverse transcription quantitative polymerase chain reaction (RT-qPCR), and the expression of BRD4 and WNT5A was detected by western blot analysis.<sup>16,17</sup>

**Isolation and identification of EVs.** The rat MSCs at passage three (serial number: SCSP-401) were cultured overnight in the serum-free Dulbecco's modified Eagle's medium (DMEM) (Merck KGaA, Darmstadt, Germany). When cell confluence reached 80% to 90%, the supernatant was collected and centrifuged at 2,000 × g for 20 minutes at 4°C to remove cell debris. The new supernatant was centrifuged at 10,000 × g for one hour at 4°C. The pellet was suspended in serum-free hydroxyethyl piperazine ethane-sulfonic acid (HEPES, 25 mm, pH = 7.4) DMEM medium and ultracentrifuged to isolate the EVs, which were stored at -80°C.<sup>18</sup>

EVs (30 µl) were dripped on a copper mesh and allowed to adhere for one minute prior to staining with phosphotungstic acid solution (30 µl, pH = 6.8). After drying under an incandescent lamp, the screens were examined under a JEOL-1400 transmission electron microscope (JEOL, Tokyo, Japan) to observe the morphology and diameter of EVs.

The content of CD63 was detected by flow cytometry using CD63-PE antibody (1:1000, ab234251; Abcam, Cambridge, Massachusetts, USA), with a blank control without primary antibody, and a type control with anti-human immunoglobulin G (IgG) labelled with polyethylene (PE). Cells were centrifuged at 1,000 rpm for five minutes and the supernatant was discarded. Cells were resuspended in phosphate-buffered saline (PBS) with 1% bovine serum albumin (BSA) and detected by Guava easyCyte system flow cytometry (Merck KGaA). Each experiment was repeated three times.

**Dorsal root ganglia neuron separation.** After rats were euthanized, the dorsal root ganglia (DRG) was isolated and its surrounding connective tissue removed by chemical dissociation with 0.125% collagenase (Ham's F12; Thermo Fisher Scientific, Waltham, Massachusetts, USA) for 1.5 hours. The DRG was then transferred to 0.25% trypsin, detached in 5% CO<sub>2</sub> and 37°C for 30

minutes, and trypsin was inactivated with 30% fetal bovine serum (FBS; Thermo Fisher Scientific). The neurones were washed three times in Ham's F12 buffer and then gently separated with a glass pipette. Neurones were seeded into 70 µm-diameter wells, with removal of clumping cells and myelin fragments by centrifugation at 9 × g for six minutes and resuspension in Ham's F12. Afterwards, the non-neuron cells were removed by centrifuging at 100 × g for ten minutes in 15% BSA. Purified DRG cells were resuspended in modified Bottenstein and Sato's medium (containing 0.1 mg/ml transferrin, 20 nM progesterone, 100 nM putrescine, 30 nM sodium selenite, 1 mg/ml BSA, 0.01 mM cytidine, and 10 pm insulin).<sup>19</sup>

**Cell culture and transfection.** MSCs (serial number: SCSP-401) and *Homo sapiens* embryonic kidney (HEK)293T cells (serial number: SCSP-502) were purchased from the cell bank of Shanghai Institute of Life Sciences, Chinese Academy of Sciences, Chinese Academy of Sciences, and cultured in DMEM medium.<sup>20</sup> DRG cells and HEK293T were cultured in DMEM medium containing 10% FBS and penicillin-streptomycin (Thermo Fisher Scientific) at 37°C and 5% CO<sub>2</sub>.<sup>20</sup> The plasmid was transfected according to the instructions of the Lipofectamine 2000 kit (Thermo Fisher Scientific). After transfection for 48 hours, the cells were collected for further experiments.<sup>21</sup>

When the DRG cells reached 80% confluence, the cells were transfected according to the instructions of Lipofectamine 2000 kit (11668 to 019; Thermo Fisher Scientific). After transfection, cells were cultured at 37°C with 5% CO<sub>2</sub> for 48 hours, whereupon the medium containing the transfection solution was discarded and then replaced with 10% FBS medium for subsequent experiments. The miR oligos and plasmids were purchased from Shanghai GenePharma (Shanghai, China). The MSCs were transfected with NC mimic, miR-381 mimic, mimic-NC/BRD4-wild type (WT), mimic-miR-381/BRD4-WT, mimic-NC/BRD4-mutant (MUT), mimic-miR-381/BRD4-MUT, oe-BRD4, si-BRD4, MSC-EV-mimic-NC, MSC-EV-miR-381 mimic, and corresponding controls, while DRG cells were transfected with oe-NC and oe-WNT5A. EVs were extracted from MSCs and co-cultured with treated DRG upon different treatments. DRG neurones were finally subjected to assays.

**BBB score.** The rats in each group were examined neurologically with the mixed single blind method on days 1, 3, 7, 14, and 28 after the injury. Crawling, the mobility of hip, knee, and ankle joints, the gait coordination ability, the body's weight-bearing ability, and the fine movement ability of the small joints in the hind limbs were recorded. The BBB score of each group was calculated for statistical analysis.

**Dual-luciferase reporter gene assay.** Dual-luciferase reporter assay was used to verify whether BRD4 is the target gene of miR-381. Plasmid Luc-BRD4-WT and mutant plasmid Luc-BRD4-MUT of BRD4 were constructed, and the Luc-BRD4-WT, miR-381, or negative control plasmids were co-transfected into HEK293T cells. After 24 hours of

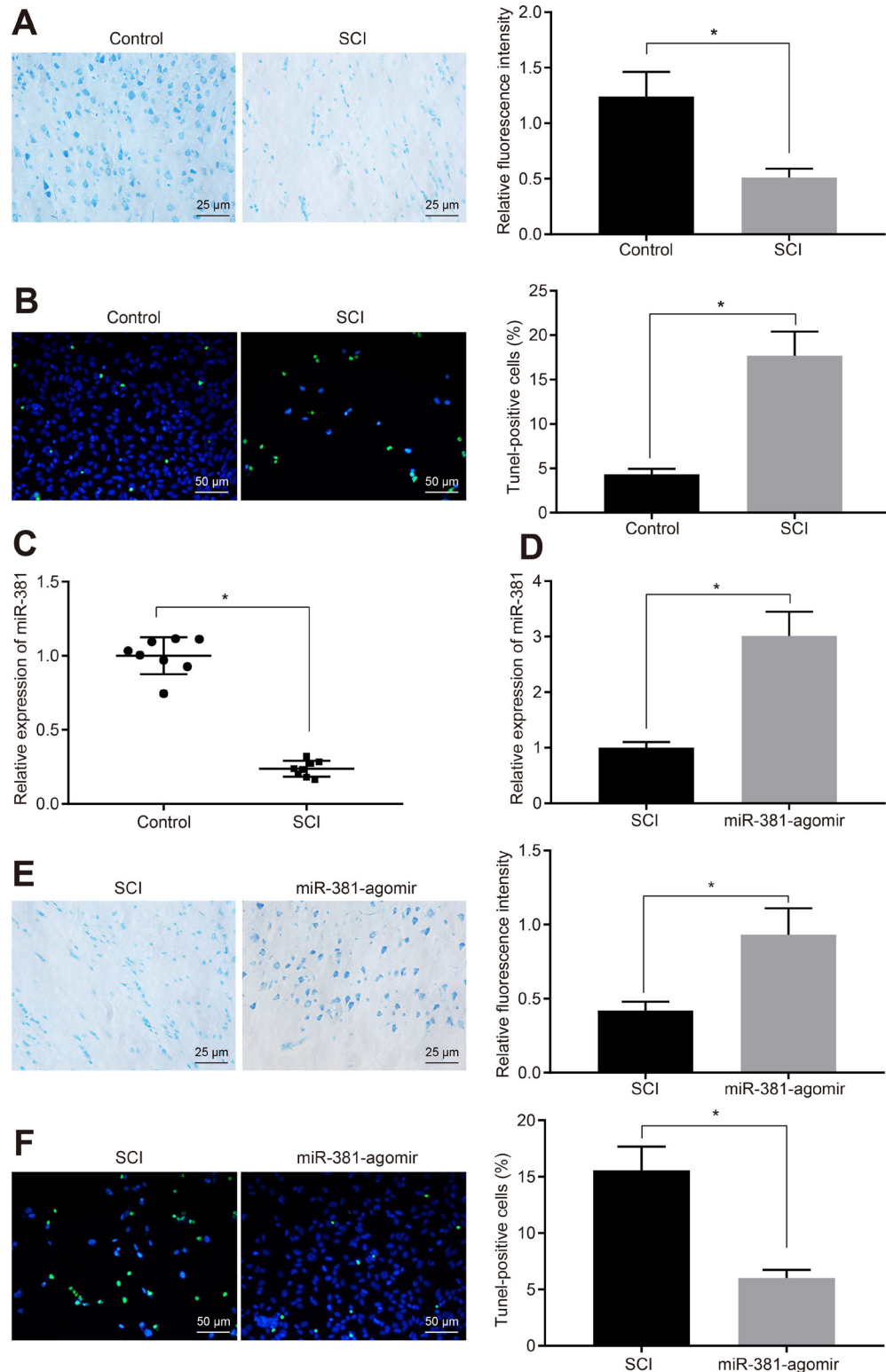


Fig. 1

MicroRNA-381 (miR-381) promoted the recovery of rats in spinal cord injury (SCI). a) The SCI model was established and Nissl staining was used to reveal the morphology of neurons (magnification 400 $\times$ ). b) The number of apoptotic cells of neurons in rat model of SCI was observed after terminal deoxynucleotidyl transferase dUTP nick end labeling (TUNEL) staining (magnification 200 $\times$ ). c) The expression of miR-381 in the SCI group and the control group was detected by quantitative reverse transcription polymerase chain reaction (RT-qPCR). d) The expression of miR-381 in SCI model treated with or without miR-381 agomir was detected. e) The cells in SCI model with or without the treatment of miR-381 agomir stained with Nissl staining (magnification 400 $\times$ ). f) TUNEL method was used to detect the apoptosis of neurons in SCI model with or without the treatment of miR-381 agomir (magnification 200 $\times$ ). \* $p < 0.05$  versus the control group in Figures 1a to 1c; \* $p < 0.05$  versus the control group in Figures 1d to 1f. Measurement data were expressed as means and SDs. The independent-samples *t*-test was used to compare the data between the two groups (eight rats).

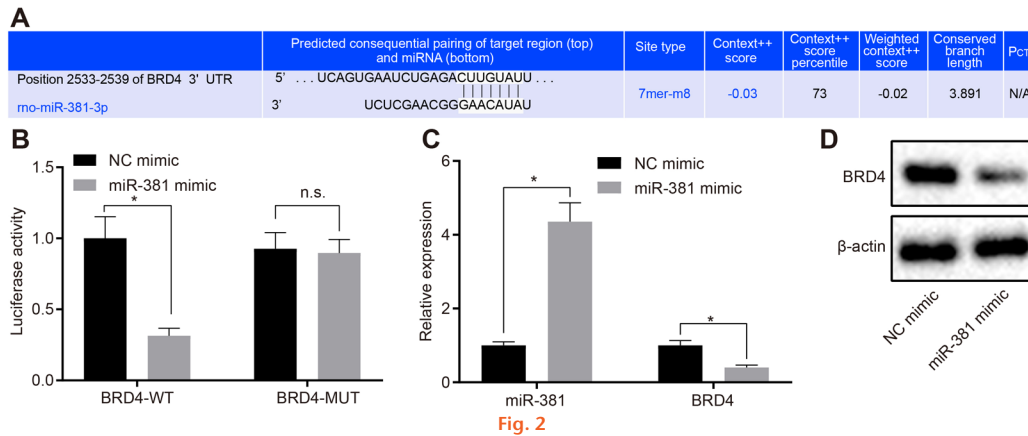


Fig. 2

MicroRNA-381 (miR-381) inhibited the expression of bromodomain-containing protein 4 (BRD4) in dorsal root ganglia (DRG) cells. a) miRNA.org was used to predict and analyze the target binding sites between miR-381 and BRD4. b) The relationship between miR-381 and three prime untranslated (3'UTR) region of BRD4 in *Homo sapiens* embryonic kidney (HEK)293T cells was detected by dual-luciferase reporter assay. c) Quantitative reverse transcription polymerase chain reaction (RT-qPCR) was used to detect the expression of miR-381 and BRD4 in DRG cells transfected with indicated plasmids. d) Western blot analysis was used to detect the expression of BRD4 in DRG cells transfected with indicated plasmids and  $\beta$ -actin was taken as internal parameter. Measurement data were expressed as means and SDs. The independent-samples *t*-test was used to compare the data between two groups. Results were representative of three individual experiments. \* $p < 0.05$  versus the NC mimic. miRNA, microRNA; n.s., not significant ( $p > 0.05$ ); PCT, conservative targeting probability.

transfection, the cells were lysed, centrifuged at 12,000 rpm for one minute, and the supernatant was collected. Luciferase activity was detected by Dual-Luciferase Reporter Assay System (E1910; Promega Corporation, Madison, Wisconsin, USA). Firefly luciferase working solution (100  $\mu$ l) was added to detect the Firefly luciferase, and Renilla luciferase working solution (100  $\mu$ l) was added to detect the Renilla luciferase. The activity of Renilla luciferase was used as internal reference, and the ratio of Firefly luciferase to Renilla luciferase was viewed as the relative luciferase activity.

**Chromatin immunoprecipitation.** The interaction between BRD4 and the enhancer region of WNT5A gene was detected by SimpleChIP Plus EnzymaticChromatin IP Kit (Cell Signalling Technology, Shanghai, China). The cells were fixed with 1% formaldehyde at room temperature for ten minutes to cross-link DNA and protein. Glycine was added to a final concentration of 0.125 mol/l to stop the reaction at room temperature for five minutes. After washing twice in precooled PBS, the cells were centrifuged at 1,600  $\times$  g for five minutes and then collected for incubation with *Micrococcus* nuclease for 20 minutes, whereupon ethylenediaminetetraacetic acid (EDTA, 50 mM) was added to stop nuclease activity. The cells were broken with an ultrasonic crusher and centrifuged at 10,000  $\times$  g for ten minutes at 4°C to separate cell debris. The supernatant was incubated with BRD4 antibody (1:1000, ab128874; Abcam) and IgG antibody (1:1000, ab6728; Abcam) overnight at 4°C. Then the mixture was centrifuged at 700 rpm for one minute. After removing the supernatant, the pellet was washed twice with 1 ml low salt buffer, high salt buffer, lithium chloride (LiCl) solution, and Tris-EDTA buffer solution, in succession. Each tube was eluted twice with 250  $\mu$ l chromatin immunoprecipitation (ChIP) Wash Buffer (Dr. Wash, Dr. Chip Biotechnology, Taipei, Taiwan). After addition of 20 ml of 5M sodium chloride (NaCl) for decrosslinking,

DNA fragments were collected. Subsequently, fluorescence quantitative PCR was used to determine the WNT5A enhancer (Forward: 5'-CGGGCCACAGTTGAGTAGTG-3'; Reverse: 5'-CGGTAATTAGGGCTTTCCAA-3') in the DNA-protein complex.

**RT-qPCR.** Trizol (Thermo Fisher Scientific) was used to extract the total RNA, and the integrity of total RNA was detected by gel electrophoresis. Absorbance at 260 nm and 280 nm was measured by Nanodrop 2000 (Thermo Fisher Scientific). Next, 1  $\mu$ g of total RNA was reversely transcribed into complementary DNA (cDNA) by PrimeScript RT reagent kit with gDNA Eraser Kit (RRO37a; Takara Holdings, Kyoto, Japan). Specific cDNA was generated by TaqMan MicroRNA reverse transcription Kit (4366596; Thermo Fisher Scientific) and then specific RT primers from TaqMan MicroRNA Assay were used to generate miR-381. The expression of miR-381 was measured by TaqMan miRNA assays according to the manufacturer instructions (Thermo Fisher Scientific). RT-qPCR was carried out on ABI7500 quantitative PCR instrument (Thermo Fisher Scientific) with SYBR Premix Ex Taq (Tli RNaseH Plus) kit (RR820a; Takara Bio, Shiga, Japan). Glyceraldehyde 3-phosphate dehydrogenase (GAPDH) was an internal reference,  $2^{-\Delta\Delta Ct}$  shows the fold change of the target gene between the experimental group and the control group, where  $\Delta\Delta Ct = Ct$  (experimental group) -  $Ct$  (control group), and  $\Delta Ct = Ct$  (gene) -  $Ct$  (internal reference).<sup>22</sup> The primers used in the experiment are shown in Table II. All primers are provided by Shanghai GenePharma.

**Western blot analysis.** Total proteins were extracted with protease inhibitors. The cells were lysed at 4°C for 15 minutes and centrifuged at 15,000 rpm for a further 15 minutes. Proteins were separated by polyacrylamide gel electrophoresis and then transferred to polyvinylidene fluoride (PVDF) membrane. After blocking in 5% BSA at room temperature for one hour, the membrane was incubated overnight at 4°C with rabbit monoclonal primary antibodies against BRD4 (1:1000,

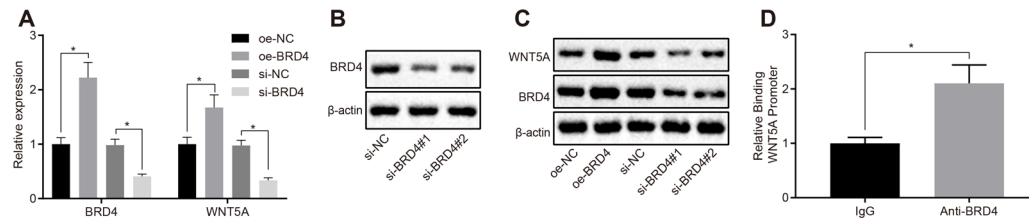


Fig. 3

Bromodomain-containing protein 4 (BRD4) promoted the expression of Wnt family member 5A (WNT5A) via binding to the promoter of WNT5A. a) Quantitative reverse transcription polymerase chain reaction (RT-qPCR) was used to detect the messenger RNA (mRNA) expression of BRD4 and WNT5A in dorsal root ganglia (DRG) cells transfected with oe-NC, oe-BRD4, silencing (si)-NC, or si-BRD4. b) Western blot analysis was used to detect the knock-down efficiency of si-BRD4. c) Western blot analysis was used to detect the protein expression of BRD4 and WNT5A in DRG cells transfected with different groups of plasmids. d) Chromatin immunoprecipitation was used to verify the binding site of BRD4 and WNT5A. \* $p < 0.05$  versus the control. Measurement data were expressed as means and SDs. The independent-samples *t*-test was used to compare the data between two groups. Data comparison among multiple groups was analyzed by one-way analysis of variance (ANOVA), followed by Tukey's post hoc test. Results were representative of three individual experiments. IgG, immunoglobulin G.

ab128874; Abcam), WNT5A (1:1000, ab238422; Abcam), CD63 (1:1000, ab217345; Abcam), CD9 (1:2000, ab92726; Abcam), CD81 (1:1000, ab109201; Abcam), GM130 (1:1000, ab52649; Abcam), or  $\beta$ -actin (1: 5000, ab179467; Abcam). The membrane was washed three times in Tris-Buffered Saline with 0.1% Tween 20 Detergent (TBST) (five minutes each time), and the samples incubated with goat monoclonal antibody to rabbit IgG (1:20,000, ab205718; Abcam) labelled with horseradish peroxidase (HRP) at room temperature for 1.5 hours. After developing by standard procedure, the ImageJ software (Bio-Rad Laboratories, Hercules, California, USA) was used for protein quantitative analysis, and the ratio of each target protein to the internal reference  $\beta$ -Actin was measured.

**Activity assay of Ras homologous A.** G-LISA Rho activity assay kit (Cytoskeleton; Denver, Colorado, USA) was used to detect the activity of Ras homologous A (RhoA) treated with WNT5A, WNT5A+Y27632 (ROCK inhibitor), or WNT5A+anti-RYK antibody. RYK can activate RhoA, a downstream effector of planar cell polarity (PCP) signalling.

**Nissl staining.** The frozen sections were air dried at room temperature for one hour and then incubated with tar violet dye solution at 60°C for one hour. The sections were washed with distilled water twice (three minutes each time), and the excess dye solution was wiped off. The sections were incubated with the differentiation solution, and then treated with ethanol series, cleared in xylene, and mounted in neutral resin. An Olympus CX23 optical microscope (Olympus America, Melville, New York, USA) was used to observe and photograph these sections.

**TUNEL staining.** Cells were fixed with 4% paraformaldehyde for 30 minutes and incubated with 0.3% hydrogen peroxide ( $H_2O_2$ )–formaldehyde solution (30%  $H_2O_2$ , volume ratio of formaldehyde = 1:99). After three rinses with PBS, cells were treated with 0.3% Triton X-100 (Pierce; Thermo Fisher Scientific) for two minutes. The terminal deoxynucleotidyl transferase dUTP nick end labeling (TUNEL) reaction mixture was prepared according to kit instructions (red fluorescence, C1089; Beyotime Institute of Biotechnology, Shanghai, China). Terminal deoxynucleotidyl transferase

(TdT) (50  $\mu$ l) and deoxyuridine triphosphate (dUTP) (450  $\mu$ l) labelled with fluorescein were mixed and added into the experimental group, while the control group received only 50  $\mu$ l of dUTP labelled with fluorescein. Cells were incubated at 37°C in the dark for one hour and washed three times with PBS. After development with anti-fluorescence quenching solution, a fluorescence microscope (BXF-100; Bingyu Optical Instrument, Shanghai, China) was used for observation with excitation wavelength 550 nm and the emission wavelength 570 nm (green fluorescence).

**Statistical analysis.** Statistical analyses were conducted using SPSS 21.0 (IBM, Armonk, New York, USA). All data were tested for normal distribution and homogeneity of variance. Measurement data were expressed by means and SDs. Data comparison among multiple groups was analyzed by one-way analysis of variance (ANOVA), followed by Tukey's post hoc test. Data of different groups at different timepoints were compared by repeated measures ANOVA, with Bonferroni post hoc testing. A *p* value < 0.05 indicated that the difference was statistically significant.

## Results

**miR-381 promoted the recovery of SCI in a rat model.** Previous studies have shown that miR-381 can alleviate SCI,<sup>21</sup> but the specific mechanism is not clear. A SCI model in rats was established, as described in the Methods section. Nissl staining showed that there was no SCI lesion in normal rats, which showed normal morphology of nerve cells and uniform distribution of Nissl granules in spinal cord tissue, and an obvious boundary of grey matter and white matter in spinal cord. However, the boundary of grey matter and white matter was unclear in SCI model rats, and neurones were shrunken and unevenly distributed (Figure 1a). The number of apoptotic neurones to TUNEL staining was significantly higher in the SCI rats compared with normal rats (Figure 1b). RT-qPCR exhibited that miR-381 was down-regulated in the SCI model rats (Figure 1c). To explore the molecular mechanism of miR-381 in the recovery of SCI, we injected miR-381-agomir into rats before modelling. The elevated expression of miR-381 in SCI rats

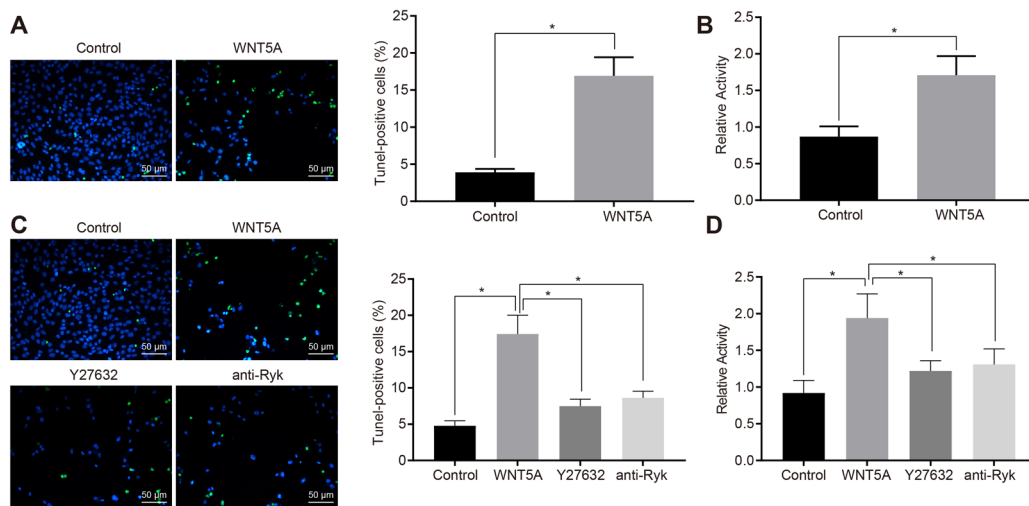


Fig. 4

Wnt family member 5A (WNT5A) promoted the apoptosis of neurons in dorsal root ganglia (DRG) cells by activating RhoA/Rho-kinase activity. a) DRG cells were treated with 90 ng/ml or without WNT5A for 24 hours. The apoptosis of DRG cells was detected by terminal deoxynucleotidyl transferase dUTP nick end labeling (TUNEL) assay (magnification 200 $\times$ ). b) DRG cells were treated with or without 90 ng/ml WNT5A for ten minutes and Rho kinase activity was detected by G-LISA Rho activity assay. c) DRG cells without any treatment and DRG cells treated with WNT5A, WNT5A + Y27632 (10  $\mu$ M; inhibited the activity of Rho-kinase), and WNT5A + anti Ryk antibody (0.5  $\mu$ g/ml) for 24 hours were tested by TUNEL staining (magnification 200 $\times$ ). d) DRG cells without any treatment and DRG cells treated with WNT5A, WNT5A + Y27632 (10  $\mu$ M) (inhibited the activity of Rho-kinase), or WNT5A + anti Ryk antibody (0.5  $\mu$ g/ml) for ten minutes were detected by G-LISA Rho activity assay. \* $p < 0.05$  versus the control. Measurement data were expressed as means and SDs. The independent-samples  $t$ -test was used to compare the data between two groups. Data comparison among multiple groups was analyzed by one-way analysis of variance (ANOVA), followed by Tukey's post hoc test. Results are derived from three separate experiments.

(Figure 1d) was rescued in rats treated with miR-381. The Nissl granules in the miR-381-agomir-treated SCI rats had a more even distribution, neuronal morphology was relatively normal (Figure 1e), and the number of apoptotic neurones was decreased (Figure 1f).

**miR-381 inhibited the expression of BRD4 in DRG cells.** To explore the mechanism of miR-381 in SCI, miRNA.org was used to predict the target gene of miRNA. We found that BRD4 was a target gene of miR-381 (Figure 2a). The dual-luciferase reporter assay confirmed that the luciferase signal of HEK293T cells co-transfected with miR-381/BRD4-WT decreased significantly ( $p < 0.05$ , Tukey's post hoc test) compared with the mimic group (Figure 2b). However, the luciferase activity in the miR-381/BRD4-MUT group did not differ when compared with the mimic-NC group ( $p > 0.05$ , Tukey's post hoc test). Thus, the three prime untranslated (3'UTR) region of BRD4 could be bound by miR-381. To investigate whether miR-381 further regulates the expression of BRD4 in DRG cells, miR-381 was overexpressed in DRG cells and the expression of miR-381 and BRD4 then detected by RT-qPCR, which confirmed up-regulated expression of miR-381 in DRG cells, whereas the mRNA expression of BRD4 was down-regulated (Figure 2c). Similarly, western blot analysis showed that protein expression of BRD4 was down-regulated in mimic-miR-381 treated DRG cells (Figure 2d). Thus, miR-381 inhibited the expression of BRD4 mRNA and protein in DRG cells by binding to the 3'UTR region of BRD4.

**BRD4 promoted the expression of WNT5A via binding to the promoter of WNT5A.** The BRD4-WNT5A axis can promote the development of breast cancer cells.<sup>13</sup> In

general, BRD4 can induce the expression of WNT5A by binding to the promoter of WNT5A, which is 2,000 base pairs (bp) target upstream of the transcription start site. To verify this mechanism in DRG cells, BRD4 was overexpressed or knocked down in DRG cells, and the mRNA and protein expression of BRD4 was detected by RT-qPCR and western blot analysis, respectively. Results showed that the mRNA and protein expression of BRD4 and WNT5A was increased when BRD4 was overexpressed. However, the mRNA and protein expression of BRD4 and WNT5A both decreased when BRD4 was knocked down (Figures 3a to 3c). These data indicate that overexpressed BRD4 upregulates the mRNA and protein expression of WNT5A. To further verify whether BRD4 can interact with the promoter of WNT5A in DRG cells, we performed a ChIP assay, which confirmed that BRD4 could bind the promoter of WNT5A (Figure 3d). Therefore, BRD4 induces the expression of WNT5A via binding to the promoter of WNT5A in DRG cells.

**WNT5A promoted the apoptosis of neurons in DRG cells by activating RhoA/Rho-kinase activity.** WNT5A reportedly inhibits the axon growth of cerebellar granule neurones in rats via effects of WNT5A binding to Ryk, a receptor involved in tyrosine kinase function, and which suppressed the recovery of SCI.<sup>14</sup> Moreover, WNT5A can stimulate cell apoptosis.<sup>23</sup> Treating DRG cells with WNT5A significantly promoted the apoptosis of DRG cells in culture (Figure 4a). At the same time, we found that increased cell-surface activity of RhoA in DRG cells that overexpress WNT5A (Figure 4b). Next, we further examined the effect of RhoA inhibitor on apoptosis in DRG cells treated with WNT5A, finding that Y27632 and

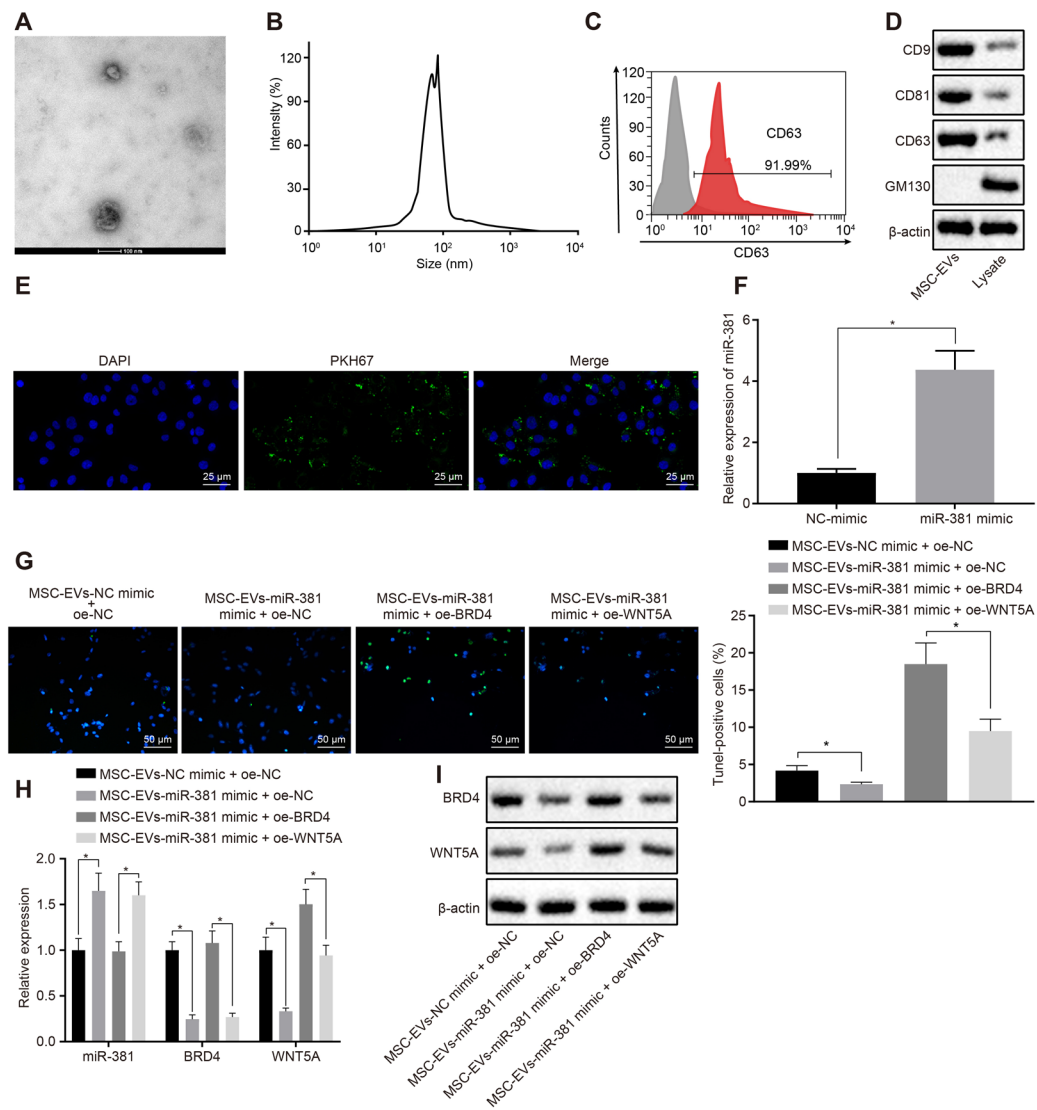


Fig. 5

Mesenchymal stem cell-derived extracellular vesicle microRNA-381 (MSC-EV-miR-381) reversed neuron apoptosis by down-regulating the bromodomain-containing protein 4 (BRD4)/Wnt family member 5A (WNT5A) axis. a) EVs were identified by transmission electron microscopy (magnification 10,000 $\times$ ). b) The diameter of EVs was detected by dynamic light scattering. c) CD63 on the surface of EVs was detected by flow cytometry. d) The protein expression of CD9, CD81, CD63, and GM130 in lysate and EVs was detected by western blot analysis. e) Representative images of EV internalization into dorsal root ganglia (DRG) cells (magnification 400 $\times$ ). f) Quantitative reverse transcription polymerase chain reaction (RT-qPCR) of miR-381 expression in cells after transfection of MSC-EV-miR-381 mimic. g) Terminal deoxynucleotidyl transferase dUTP nick end labelling (TUNEL) staining of apoptosis of DRG cells upon treatment with MSC-EV-NC mimic  $\pm$  oe NC; MSC-EV-miR-381 mimic  $\pm$  oe NC; MSC-EV-NC mimic  $\pm$  oe-WNT5A; MSC-EV-miR-381 mimic  $\pm$  oe-WNT5A (magnification 200 $\times$ ). h) RT-qPCR of miR-381, BRD4, and WNT5A expression in DRG cells upon treatment of MSC-EV-NC mimic + oe NC; MSC-EV-miR-381 mimic + oe NC; MSC-EV-NC mimic + oe-WNT5A; MSC-EV-miR-381 mimic + oe-WNT5A. i) Western blot analysis of BRD4 and WNT5A in DRG cells upon treatment with MSC-EV-NC mimic + oe NC, MSC-EV-miR-381 mimic + oe NC, MSC-EV-NC mimic + oe-WNT5A, or MSC-EV-miR-381 mimic + oe-WNT5A. \* $p < 0.05$  versus MSC-EV-NC mimic+oe NC treatment. The data in the figure are all measurement data, which are expressed as mean and SDs from three separate experiments. The independent-samples *t*-test was used to compare the data between two groups.

anti-Ryk antibodies could both alleviate the effect of WNT5A on DRG apoptosis (Figure 4c), and that Y27632 and anti-Ryk antibodies could inhibit the activity of RhoA (Figure 4d). Thus, WNT5A can promote apoptosis in DRG cells by activating RhoA/Rho-kinase activity, and Y27632 and anti-Ryk antibodies can inhibit apoptosis effect of WNT5A on DRG cells. **miR-381 derived from EVs in MSCs reversed neuron apoptosis through down-regulating BRD4/WNT5A axis.** To investigate the effect of miR-381 derived from EVs in

MSCs on SCI, we isolated EVs followed by observation under a transmission electron microscope. We found that the EVs were round or elliptic membranous vesicles with similar morphology (Figure 5a). The diameter of EVs as detected by dynamic light scattering was in the range of 30 nm to 120 nm (Figure 5b). Flow cytometry detecting the surface marker CD63 on EVs (Figure 5c) showed that more than 90% of the events were CD63-positive. In addition, other exosome markers in EVs,

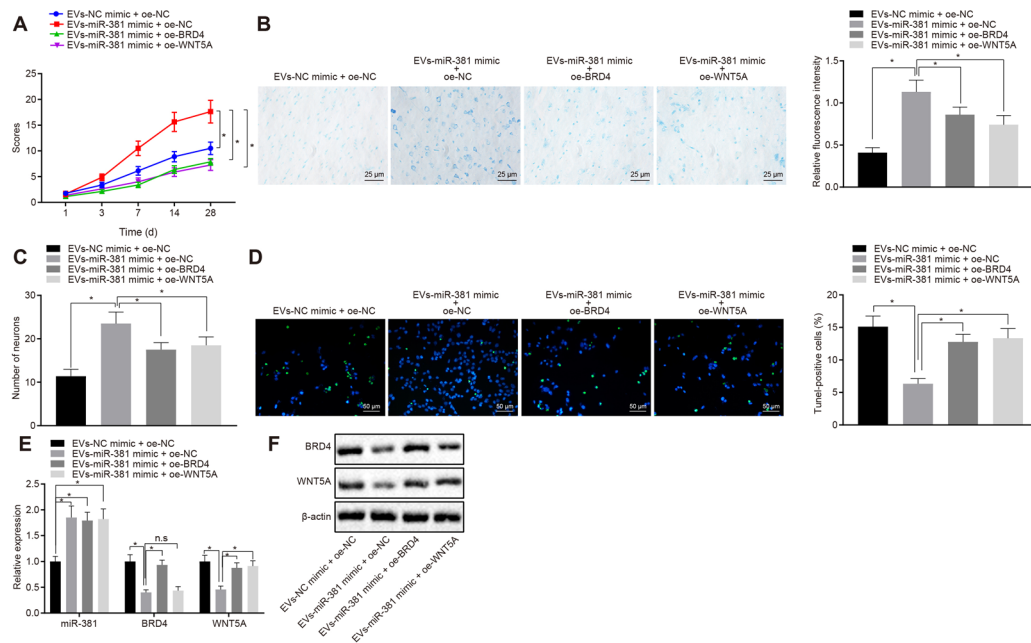


Fig. 6

MicroRNA-381 (miR-381) derived from extracellular vesicles (EVs) in mesenchymal stem cells (MSCs) promoted the recovery of spinal cord injury (SCI) by inhibiting bromodomain-containing protein 4 (BRD4)/Wnt family member 5A (WNT5A) axis. a) The Basso, Beattie and Bresnahan locomotor rating scale (BBB) scores were recorded in three rats in each group at 1, 3, 7, 14, and 28 days by the mixed single blind method (MSC-EV-NC mimic+oe NC; MSC-EV-miR-381 mimic+oe NC; MSC-EV-NC mimic+oe-WNT5A; MSC-EV-miR-381 mimic+oe-WNT5A). b) The spinal cord tissues of rats were observed by Nissl staining and the fluorescence intensity was measured (magnification 400 $\times$ ). c) The number of motoneurons in spinal cord of rats was counted by Nissl staining. d) The apoptosis in neurons was observed by terminal deoxynucleotidyl transferase dUTP nick end labeling (TUNEL) staining (magnification 200 $\times$ ). e) RT-qPCR of miR-381, BRD4, and WNT5A expression in rats upon treatment with MSC-EV-NC mimic+oe NC; MSC-EV-miR-381 mimic+oe NC; MSC-EV-NC mimic+oe-WNT5A; MSC-EV-miR-381 mimic+oe-WNT5A. f) Western blot analysis of BRD4 and WNT5A protein expression upon treatment with MSC-EV-NC mimic+oe NC, MSC-EV-miR-381 mimic+oe NC, MSC-EV-NC mimic+oe-WNT5A, or MSC-EV-miR-381 mimic+oe-WNT5A. \* $p < 0.05$  versus NC mimic+oe NC treatment. Measurement data were expressed as means and SDs ( $n = 8$ ). Data comparison among multiple groups was analyzed by one-way analysis of variance (ANOVA), followed by Tukey's post hoc test. Data of different groups at different timepoints were compared by repeated measures ANOVA with Bonferroni correction.

such as CD9, CD81, CD63, and GM130 were detected by western blot analysis, all of which confirmed the successful isolation of EVs of high purity (Figure 5d).

To validate whether DRG cells can be transferred as EV cargo, EVs labelled with PKH67 (green) were co-cultured with DRG cells for 48 hours. The uptake of EVs in DRG cells was observed under a confocal fluorescence microscope, which showed conspicuous uptake of EVs labelled with PKH67 in DRG cells at 48 hours, confirming that EVs can be transferred from MSCs into DRG cells (Figure 5e). We found that miR-381 was highly expressed in EVs of MSC cells transfected with miR-381 mimic (Figure 5f). To explore the effect of miR-381 in EVs in DRG cells, we co-cultured EVs with DRG cells that overexpressed WNT5A. Results depicted that overexpressed WNT5A can facilitate apoptosis in neurones, while overexpressed miR-381 can reverse the promotive effect of WNT5A on this apoptosis (Figure 5g). The expression of miR-381, BRD4, and WNT5A in neurones of DRG cells was detected by RT-qPCR and western blot analysis. Results indicated that overexpressed WNT5A had no impact on the expression of miR-381 and BRD4 in DRG cells, but overexpressed miR-381 inhibited the mRNA and protein expression of BRD4 and WNT5A in

DRG cells (Figures 5h and 5i). To sum up, our study showed that miR-381 derived from EVs in MSCs can reverse neuron apoptosis by down-regulating the BRD4/WNT5A axis.

**miR-381 derived from EVs in MSCs promoted the recovery of SCI through inhibiting BRD4/WNT5A axis.** The SCI rats were assessed by the BBB score, which increased significantly between one and 14 days post injury, and was relatively stable between 14 and 28 days in the EV-NC mimic+ overexpression (oe) NC group. The recovery of the rats in the early stage in the EV-miR-381 mimic+oe NC group was faster than that in the EV-miR-381 mimic+oe-BRD4 group and the EV-miR-381 mimic+oe-WNT5A groups. At 14 days post-model induction, the muscle strength in the EV-miR-381 mimic+oe NC group was significantly restored, the hind limbs could be contracted with supporting force, and the abdomen could be elevated, with signs of returning balance, coordination, and fine motor ability. These data indicated better recovery than in the other three treatment groups at between seven and 28 days (Figure 6a). Nissl staining was used to observe the motoneurons in the anterior horn of the spinal cord in the rats, and the number of motoneurons was counted (Figures 6b and 6c). In the

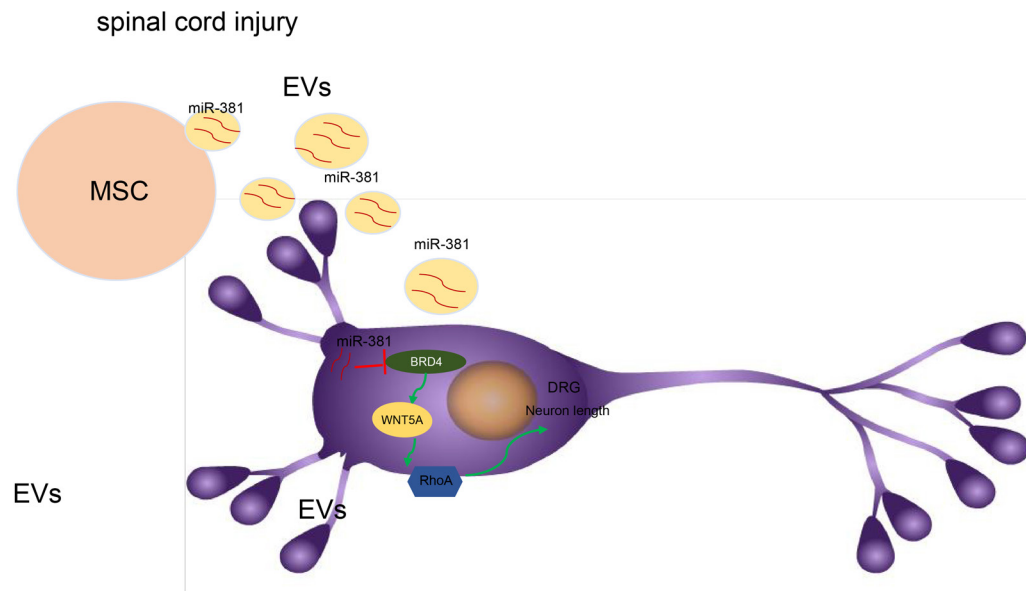


Fig. 7

Mechanism diagram illustrating that microRNA-381 (miR-381) can activate Ras homologous A (RhoA)/Rho-kinase activity to promote the apoptosis of neurones in dorsal root ganglia (DRG) cells by inhibiting bromodomain-containing protein 4 (BRD4). Moreover, miR-381 derived from extracellular vesicles (EVs) in mesenchymal stem cells (MSCs) promoted the recovery of spinal cord injury (SCI) by inhibiting the BRD4/Wnt family member 5A (WNT5A) axis in a rat model.

EV-NC mimic+oe NC group, the boundary between white matter and grey matter of the spinal cord was unclear, there were few motoneurons in the grey matter area, and those that remained were shrunken and unevenly distributed, with disordered distribution of Nissl granules. In the EV-miR-381 mimic+oe NC group, there was a clear boundary of grey matter and white matter in the anterior horn of spinal cord, but the morphology of grey matter had changed, containing slightly swollen structures and numerous motoneurons with even distributions of Nissl granules. In the EV-miR-381 mimic+oe-BRD4 and the EV-miR-381 mimic+oe-WNT5A groups, the loss of motoneurons in grey matter was intermediate to that seen in the EV-mimic+oe NC and EV-miR-381 mimic+oe NC groups. TUNEL staining results indicated that miR-381 can inhibit the apoptosis of neurons in SCI mode, which was counteracted by overexpressed BRD4 and WNT5A (Figure 6d). RT-qPCR showed that the expression of miR-381 significantly increased in the spinal cord of rats injected with EVs containing miR-381. Overexpressed BRD4 upregulated mRNA expression of WNT5A but did not affect expression of miR-381. Overexpressed WNT5A had no effect on the RNA expression of miR-381 and BRD4 (Figure 6e). Western blot analysis showed that miR-381 can inhibit protein expression of BRD4 and WNT5A, and overexpressed BRD4 also stimulated protein expression of WNT5A. However, overexpressed WNT5A exerted no influence on expression of BRD4 (Figure 6f). Thus, our study demonstrated that miR-381 derived from EVs from MSCs promoted the recovery of SCI by mediating the BRD4/WNT5A axis.

## Discussion

EVs can be regarded as a vehicle to convey bioactive molecules to target cells, and thus EVs derived from various cells have been reported to be a potential therapeutic method for treating different diseases.<sup>24</sup> MicroRNAs are known to exert a notable influence on many disorders, such as neuroinflammation, cell apoptosis, and axon regeneration.<sup>25</sup> Though one study indicated that miR-381 can play a beneficial role in the treatment of SCI,<sup>10</sup> there was no further research on the relationship between miRNAs and SCI. Therefore, we aimed in this study to discern the role and function of miR-381 and its downstream target genes, BRD4 and WNT5A, in SCI. The data from this study support a conclusion that miR-381 derived from EVs in MSCs promotes the recovery of SCI by inhibiting BRD4/WNT5A (Figure 7).

Bone marrow MSCs generate various types of cells due to their broad differentiative capacity and self-renewal, and are consequently highlighted for their potential use in bone regenerative medicine and neurological diseases such as SCI.<sup>26–28</sup> MSCs are regulated by various factors: for example, Angelica polysaccharide promotes proliferation, cycle progression, and osteoblast differentiation in MSCs.<sup>29</sup> The addition of parathyroid hormone strengthens the characteristics of osteogenic and adipogenic differentiation of MSCs.<sup>29</sup> MSCs are known as a promising source of therapeutic EVs, while they are popular targets for developing new therapeutic procedures in various diseases.<sup>30</sup> For example, miR-21 was delivered to neurons by rat bone marrow MSCs, suppressing apoptosis and promoting spinal cord repair.<sup>31</sup> A notable finding in our study was that miR-381 derived from EVs in

MSCs inhibited the expression of BRD4 in DRG neurons. Functions of EVs include intercellular transfer and protein transmission in the recipient cell.<sup>7</sup> Additionally, miRNA in EVs from stem cells can have a protective effect in the experimental therapy for acute kidney injury.<sup>32</sup> Specifically, by down-regulating CXCR4, miR-381 can promote the proliferation of renal tubular epithelial cells following renal ischaemia reperfusion injury.<sup>33</sup> High expression of miR-381 played a promotive role in cell proliferation as well as inhibition of neurocyte apoptosis and the expression of relative proteins in SCI.<sup>10</sup> Furthermore, BRD4 was predicted to be the target gene of miR-381, and we confirmed this prediction using miRNA.org and dual-luciferase reporter assay.

Another finding of our study was that EV-derived miR-381 in MSCs can promote the recovery of SCI through inhibition of the BRD4/WNT5A axis. BRD4 plays a key role in cell proliferation, differentiation, and gene transcription.<sup>34</sup> Down-regulated BRD4 suppresses cell apoptosis and alleviates endoplasmic reticulum stress caused by renal ischaemia/reperfusion injury through FoxO4. These findings offer a potential new avenue for the treatment of renal injury.<sup>35</sup> Meanwhile, a previous study verified that BRD4 expression in SCI was increased to an extent correlating with BRD4 downregulation, which could alleviate inflammatory microglial reactions and thus promote recovery from SCI.<sup>16</sup> Similarly, overexpressed miR-381 can promote the repair of nerve injury following acute cerebral ischaemia through its activation of the SDF-1/CXCR4 pathway via LRRC4.<sup>36</sup> Another study showed that miR-381 was a diagnostic biomarker for viral myocarditis and held promise for the treatment of myocardial cell damage, while also protecting functions of myocardial cells in children and mice through its anti-inflammatory effects on COX-2.<sup>37</sup> Other evidence indicates that WNT5A is involved in neuropathic pain caused by nerve injury.<sup>38</sup> Previous evidence has revealed that WNT5A is essential for the inflammatory response of macrophages in humans and also emerged as a target for activated protein C or soluble frizzled-related peptide-1.<sup>39</sup> Consistent with this general scenario, inhibition of BRD4 reduced WNT5A expression, suppressing malignant phenotypes of breast cancer cells.<sup>13</sup>

In conclusion, we found that miR-381 delivered by EVs from MSCs facilitates the recovery of SCI in rat models, which provides a novel perspective for the improved treatment of SCI. However, future studies will aim at developing a better understanding of miR-381 and genes involved in SCI and other diseases.

## References

1. **National Spinal Cord Injury Statistical Center.** Spinal cord injury facts and figures at a glance. *J Spinal Cord Med.* 2014;37(1):117–118.
2. **Silva NA, Sousa N, Reis RL, Salgado AJ.** From basics to clinical: a comprehensive review on spinal cord injury. *Prog Neurobiol.* 2014;114:25–57.
3. **Villegas-Amtmann S, Atkinson S, Paras-Garcia A, Costa DP.** Seasonal variation in blood and muscle oxygen stores attributed to diving behavior, environmental temperature and pregnancy in a marine predator, the California sea lion. *Comp Biochem Physiol A Mol Integr Physiol.* 2012;162(4):413–420.
4. **Varma AK, Das A, Wallace G, Gt W, et al.** Spinal cord injury: a review of current therapy, future treatments, and basic science frontiers. *Neurochem Res.* 2013;38(5):895–905.
5. **Stephan K, Huber S, Häberle S, et al.** Spinal cord injury—incidence, prognosis, and outcome: an analysis of the TraumaRegister DGU. *Spine J.* 2015;15(9):1994–2001.
6. **Shende P, Subedi M.** Pathophysiology, mechanisms and applications of mesenchymal stem cells for the treatment of spinal cord injury. *Biomed Pharmacother.* 2017;91:693–706.
7. **Tetta C, Ghigo E, Silengo L, Deregibus MC, Camussi G.** Extracellular vesicles as an emerging mechanism of cell-to-cell communication. *Endocrine.* 2013;44(1):11–19.
8. **Ferreira E, Porter RM.** Harnessing extracellular vesicles to direct endochondral repair of large bone defects. *Bone Joint Res.* 2018;7(4):263–273.
9. **Zafari S, Backes C, Leidinger P, Meese E, Keller A.** Regulatory microRNA networks: complex patterns of target pathways for disease-related and housekeeping microRNAs. *Genomics Proteomics Bioinformatics.* 2015;13(3):159–168.
10. **Ruan W, Ning G, Feng S, Gao S, Hao Y.** MicroRNA-381/Hes1 is a potential therapeutic target for spinal cord injury. *Int J Mol Med.* 2018;42(2):1008–1017.
11. **Yuan B, Pan S, Dong Y-Q, Zhang W-W, He X-D.** Effect of exosomes derived from mir-126-modified mesenchymal stem cells on the repair process of spinal cord injury in rats. *Eur Rev Med Pharmacol Sci.* 2020;24(2):483–490.
12. **Truong H-HM, Fatch R, Tan JY, Raymond HF, McFarland W.** Whose responsibility is it? beliefs about preventing HIV transmission among men who have sex with men. *Sex Transm Dis.* 2018;45(7):e43–e48.
13. **Shi J, Wang Y, Zeng L, et al.** Disrupting the interaction of BRD4 with diacetylated twist suppresses tumorigenesis in basal-like breast cancer. *Cancer Cell.* 2014;25(2):210–225.
14. **Miyashita T, Koda M, Kitajo K, et al.** Wnt-Ryk signaling mediates axon growth inhibition and limits functional recovery after spinal cord injury. *J Neurotrauma.* 2009;26(7):955–964.
15. **Song RB, Basso DM, da Costa RC, Fisher LC, Mo X, Moore SA.** Adaptation of the Basso-Beattie-Bresnahan locomotor rating scale for use in a clinical model of spinal cord injury in dogs. *J Neurosci Methods.* 2016;268:117–124.
16. **Wang J, Chen J, Jin H, et al.** Brd4 inhibition attenuates inflammatory response in microglia and facilitates recovery after spinal cord injury in rats. *J Cell Mol Med.* 2019;23(5):3214–3223.
17. **Zhou X, Chu X, Yuan H, et al.** Mesenchymal stem cell derived EVs mediate neuroprotection after spinal cord injury in rats via the microRNA-21-5p/FasL gene axis. *Biomed Pharmacother.* 2019;115:108818.
18. **Zhang G, Zou X, Miao S, et al.** The anti-oxidative role of micro-vesicles derived from human Wharton-Jelly mesenchymal stromal cells through NOX2/gp91(phox) suppression in alleviating renal ischemia-reperfusion injury in rats. *PLoS One.* 2014;9(3):e92129.
19. **Gardiner NJ, Fernyhough P, Tomlinson DR, Mayer U, von der Mark H, Streuli CH.** Alpha7 integrin mediates neurite outgrowth of distinct populations of adult sensory neurons. *Mol Cell Neurosci.* 2005;28(2):229–240.
20. **Gaudet AD, Mandrekar-Colucci S, Hall JCE, et al.** miR-155 deletion in mice overcomes Neuron-Intrinsic and Neuron-Extrinsic barriers to spinal cord repair. *J Neurosci.* 2016;36(32):8516–8532.
21. **Chen W-C, Luo J, Cao X-Q, Cheng X-G, He D-W.** Overexpression of miR-381-3p promotes the recovery of spinal cord injury. *Eur Rev Med Pharmacol Sci.* 2018;22(17):5429–5437.
22. **Livak KJ, Schmittgen TD.** Analysis of relative gene expression data using real-time quantitative PCR and the 2(-Delta Delta C(T)) Method. *Methods.* 2001;25(4):402–408.
23. **Peng S, Zhang J, Chen J, Wang H.** Effects of Wnt5a protein on proliferation and apoptosis in JAR choriocarcinoma cells. *Mol Med Rep.* 2011;4(1):99–104.
24. **György B, Hung ME, Breakefield XO, Leonard JN.** Therapeutic applications of extracellular vesicles: clinical promise and open questions. *Annu Rev Pharmacol Toxicol.* 2015;55:439–464.
25. **Yan H, Hong P, Jiang M, Li H.** Micromas as potential therapeutics for treating spinal cord injury. *Neural Regen Res.* 2012;7(17):1352–1359.
26. **Alishahi M, Anbiyaiee A, Farzaneh M, Khoshnam SE.** Human mesenchymal stem cells for spinal cord injury. *Curr Stem Cell Res Ther.* 2020;15(4):340–348.
27. **Marolt Presen D, Traweger A, Gimona M, Redl H.** Mesenchymal stromal cell-based bone regeneration therapies: from cell transplantation and tissue engineering to therapeutic secretomes and extracellular vesicles. *Front Bioeng Biotechnol.* 2019;7:352.
28. **Witwer KW, Van Balkom BWM, Bruno S, et al.** Defining mesenchymal stromal cell (MSC)-derived small extracellular vesicles for therapeutic applications. *J Extracell Vesicles.* 2019;8(1):1609206.

29. **Xie X, Liu M, Meng Q.** Angelica polysaccharide promotes proliferation and osteoblast differentiation of mesenchymal stem cells by regulation of long non-coding RNA H19. *Bone Joint Res.* 2019;8(7):323–332.
30. **Bianco P, Cao X, Frenette PS, et al.** The meaning, the sense and the significance: translating the science of mesenchymal stem cells into medicine. *Nat Med.* 2013;19(1):35–42.
31. **Kang J, Li Z, Zhi Z, Wang S, Xu G.** Mir-21 derived from the exosomes of MscS regulates the death and differentiation of neurons in patients with spinal cord injury. *Gene Ther.* 2019;26(12):491–503.
32. **Livingston MJ, Wei Q.** MicroRNAs in extracellular vesicles protect kidney from ischemic injury: from endothelial to tubular epithelial. *Kidney Int.* 2016;90(6):1150–1152.
33. **Zheng G-H, Wen X, Wang Y-J, et al.** MicroRNA-381-induced down-regulation of CXCR4 promotes the proliferation of renal tubular epithelial cells in rat models of renal ischemia reperfusion injury. *J Cell Biochem.* 2018;119(4):3149–3161.
34. **Taniguchi Y.** The bromodomain and extra-terminal domain (BET) family: functional anatomy of BET paralogous proteins. *Int J Mol Sci.* 2016;17(11):1849.
35. **Liu H, Wang L, Weng X, et al.** Inhibition of BRD4 alleviates renal ischemia/reperfusion injury-induced apoptosis and endoplasmic reticulum stress by blocking FoxO4-mediated oxidative stress. *Redox Biol.* 2019;24:101195.
36. **Xue Y, Xu T, Jiang W.** Dexmedetomidine protects PC12 cells from ropivacaine injury through miR-381/LRRC4 /SDF-1/CXCR4 signaling pathway. *Regen Ther.* 2020;14(14):322–329.
37. **Zhang Y, Sun L, Sun H, et al.** MicroRNA-381 protects myocardial cell function in children and mice with viral myocarditis via targeting cyclooxygenase-2 expression. *Exp Ther Med.* 2018;15(6):5510–5516.
38. **Wang J, Zhang S, Li L, Zhang L.** Involvement of Wnt5a within the cerebrospinal fluid-contacting nucleus in nerve injury-induced neuropathic pain. *Int J Neurosci.* 2015;125(2):147–153.
39. **Pereira C, Schaer DJ, Bachli EB, Kurrer MO, Schoedon G.** Wnt5A/CaMKII signaling contributes to the inflammatory response of macrophages and is a target for the antiinflammatory action of activated protein C and interleukin-10. *Arterioscler Thromb Vasc Biol.* 2008;28(3):504–510.

**Author information:**

- X. Jia, MM, Attending Doctor
- G. Huang, MD, Associate Senior Doctor
- S. Wang, MM, Attending Doctor
- M. Long, MB, Supervisor Nurse
- X. Tang, MB, Chief Physician  
The People's Hospital of Jianyang City, Jianyang, China.
- D. Feng, MB, Professor
- Q. Zhou, MD, Chief Physician  
The Affiliated Hospital of Southwest Medical University, Luzhou, China.

**Author contributions:**

- X. Jia: Designed the study, Collated the data, Carried out the data analyses, Drafted the manuscript.
- G. Huang: Designed the study, Collated the data, Carried out the data analyses, Drafted the manuscript.
- S. Wang: Designed the study, Collated the data, Carried out the data analyses, Drafted the manuscript.
- M. Long: Designed the study, Collated the data, Carried out the data analyses, Drafted the manuscript.
- X. Tang: Designed the study, Collated the data, Carried out the data analyses, Drafted the manuscript.
- D. Feng: Designed the study, Collated the data, Carried out the data analyses, Drafted the manuscript.
- Q. Zhou: Designed the study, Collated the data, Carried out the data analyses, Drafted the manuscript.

**Funding statement:**

- This study was supported by the Medical Research Project of Chengdu in 2017 (No. 2017091), the Project of Sichuan Department of Science and Technology (No. 2016PJ552), and the Project of Luzhou Department of Science and Technology (No. 2016-R-70(18/24)). The authors choose not to provide any additional funding statements.

**Acknowledgements:**

- We would like to give our sincere appreciation to the reviewers for their helpful comments on this article.

**Ethical review statement:**

- The animal experiments in this study were conducted under the approval of the Animal Ethics Committee in The Affiliated Hospital of Southwest Medical University, in strict consideration of the need to minimize discomfort and animal numbers.

© 2021 Author(s) et al. This is an open-access article distributed under the terms of the Creative Commons Attribution Non-Commercial No Derivatives (CC BY-NC-ND 4.0) licence, which permits the copying and redistribution of the work only, and provided the original author and source are credited. See <https://creativecommons.org/licenses/by-nc-nd/4.0/>.